Journal of Magnetic Resonance 304 (2019) 35–41

Contents lists available at ScienceDirect

Journal of Magnetic Resonance

journal homepage: www.elsevier.com/locate/jmr

A low cost, portable NMR probe for high pressure, MR relaxometry ☆

Julia D. Kerr [a], Bruce J. Balcom [b], Michael J. McCarthy [a], Matthew P. Augustine [a,*]

[a] Department of Chemistry, 69 Chemistry Building, University of California, Davis, Davis, CA 95616 USA
[b] Department of Physics, UNB MRI Centre, University of New Brunswick, Fredericton, New Brunswick, Canada

ARTICLE INFO

Article history:
Received 1 March 2019
Revised 2 May 2019
Accepted 2 May 2019
Available online 2 May 2019

Keywords:
High pressure
Portable NMR
Relaxometry
Single sided magnets

ABSTRACT

A low cost, portable, high volume, stainless steel pressure reactor is modified to easily perform magnetic resonance relaxometry at industrially relevant pressures. Unlike existing pressurization strategies common to nuclear magnetic resonance (NMR) spectroscopy, this approach is amenable to realistic samples that feature heterogeneity and have traditionally escaped NMR study at pressure. This pressure reactor/NMR probe combination is easily accommodated by most single-sided and other low magnetic field permanent magnet assemblies. The performance of the probe is demonstrated by accomplishing NMR relaxometry on polydimethylsiloxane at different pressures with two types of unilateral magnets.

1. Introduction

Liquid and solid state nuclear magnetic resonance (NMR) spectroscopy have enjoyed a rich history in the characterization of material properties and chemical transformations at elevated pressure. The pioneering work of Jonas in the development of NMR probes with hydraulic based pressure cells enabled the initial NMR characterization of liquids at pressures up to 900 MPa [1]. Originally this type of high pressure NMR research was restricted to those with access to the pressurization apparatus and NMR probes of the Jonas design [1–3]. The situation has improved in the past few years as Daedelus Innovations improved on the Jonas approach to produce a commercially available pressure cell and necessary pressurization hardware [4]. The Daedelus device uses a zirconia cell to replace a standard 5 mm NMR tube that can be accommodated by most high resolution NMR probes, a feature that lead Wand to study pressure recyclable protein folding with high resolution NMR [5]. The protein folding work is remarkable, but the time scale of pressurization limits the study to equilibrium chemical structure changes with and without added pressure [6]. Recently, Bax replaced the low volume syringe pump pressurization apparatus with a large volume bellows system to enable the zirconia cell enclosed sample pressure to drop by ca. 200 MPa in ca. 2 ms, thus allowing the measurement of real time pressure induced folding dynamics by NMR [7].

The hydraulic based pressurization strategies are limited to pressures below about 900 MPa [1] which is adequate for protein folding research, but far too low to study other problems requiring much higher pressure, like aqueous phase geochemistry [8,9]. To achieve these higher pressures, mechanical force is used. For liquids, Casey developed a clamp cell based NMR probe capable of delivering high resolution, two dimensional, liquid state NMR spectra for solutes in water or organic solvent at pressures up to 3 GPa [10]. Simple modifications to the coil orientation and the exotic alloys used in the probe construction will easily increase the operating pressure upper limit to 5 GPa. An attractive feature of the clamp cell design is that the sample volume is kept ca. 1 mL, thus examination of solute and heteronuclei NMR spectra at pressures up to 5 GPa is possible. Two orders of magnitude higher pressure has been mechanically established on nL volume samples with diamond anvil cells modified for NMR spectroscopy [11]. Both the clamp cell and diamond anvil based NMR probes are custom built research devices that are not commercially available.

The goal of this work was to develop a low cost, portable NMR probe capable of studying realistic, heterogeneous, industrially relevant, sometimes reactive, samples at elevated pressure. Realistic samples include food, biomass, drilling muds, etc. that are not usually homogeneously dispersed. Unfortunately, available high pressure NMR instrumentation designs are not amenable to this type of research. Current approaches to high pressure NMR have focused

☆ This research did not receive any specific grant from funding agencies in the public, commercial, or not-for-profit sectors.

* Corresponding author.
E-mail address: maugust@ucdavis.edu (M.P. Augustine).

https://doi.org/10.1016/j.jmr.2019.05.001
1090-7807/

on the pressurized space being enclosed in the magnet. Having the pressurized sample enclosed in a magnet assigns a geometric and size limit to the probe and pressurization system. The small physical size requirement translates into the development of delicate, expensive, equipment with a small sample volume. Other custom approaches have demonstrated that NMR is feasible in conjunction with metallic, high pressure vessels that have the coils located inside the pressure space with the vessel acting as the ground shield, as discussed below [12,13]. These other approaches are restricted to either lower pressures or specific samples and geometries like cylindrical rock cores [12–14]. The low volume of existing approaches is the first problem. Although adequate for limited quantity biomolecule solutions, the low nL – mL sample volumes of existing NMR pressure cells make the study of many realistic samples at pressure impossible i.e. it is difficult to load an oil sample with small rocks or paste, like guacamole, into a valuable, 3 mm inner diameter, zirconia NMR pressure cell. A second problem is durability. Commercially available and research specific NMR pressure devices are designed for use in academic laboratories where simple two component clean solutions are used. Industrially relevant dirty mixtures will significantly reduce the lifetime of the existing pressure cells. Finally, there is cost. The Daedelus liquids and the diamond anvil cell solids pressurization hardware involves expensive components, thus much high pressure research is expensive to accomplish.

The samples of interest to this work are realistic, meaning that they are mixtures of chemical compounds and/or mixtures of liquids and solids. As most of these samples are also industrially relevant, a maximum operating pressure of at most 600 MPa, or 87 Kpsi, is required. This pressure is consistent with the operating pressure of most modern high pressure food processors [15]. Since such samples often lead to congested, largely uninterpretable NMR spectra there is no need to use expensive, high resolution magnets for this work. NMR relaxometry, on the other hand, has a rich history in the characterization of realistic samples, does not require expensive magnets and can consequently be accomplished anywhere a portable magnet is placed.

Marble et al., in 2007, introduced a three magnet array, single sided portable magnet [16]. The design is simple, small and compact with a homogeneous sweet spot ca. 1 cm from the magnet surface. In 2014, García-Naranjo et al. showed that this magnet array could be used in conjunction with a solenoid coil to produce reliable relaxometry measurements on rock core samples with elongated, challenging geometries. Utsuzawa and Fukushima in 2017, described an alternative cylindrical unilateral magnet that uses a magnetic field saddle point to create adequate field homogeneity. This cylindrical barrel magnet was used to obtain T_1 weighted magnetic resonance images of whole coconuts and to track tomato concentrate spoilage in sealed 1000 L containers [18]. These efforts demonstrate that portable NMR reliably accommodates challenging, non-traditional sample geometries. This work considers adapting commercially available pressure reactors to two portable single sided magnets to accomplish variable pressure MR relaxometry. Some advantages of this approach are that temperature and flow can be easily controlled and introduced.

The pressure reactors from High Pressure Equipment Company (HiP) are inexpensive, readily available, and specifically designed to study realistic samples at pressures up to 1000 MPa. The following pages describe how a HiP, MS – 17 micro series pressure reactor is modified with a drill and simple components to make a robust, durable, low cost NMR probe to accomplish pressure dependent relaxometry with portable magnets. After describing these modifications, the performance of the new HiP-NMR probe is demonstrated by measuring ^{1}H relaxation time correlation data as a function of pressure for polydimethylsiloxane (PDMS) with two different unilateral, single sided magnets.

2. The HiP-NMR probe

The key design feature that allows for simple modification of a commercial off the shelf pressure reactor for NMR measurements is a mixture of Stycast epoxy with Al_2O_3 powder. Since this mixture reliably seals small NMR detection coil lead holes in Berylco-25 alloy up to applied pressures of 3 GPa, the same approach is used here. A standard 316 stainless steel MS – 17 micro reactor, essentially a 1 in. outer diameter, 9/16 in. inner diameter stainless steel tube with threaded ends, and two stainless steel endcaps were purchased from HiP. One of the stainless steel endcaps (Part No. 20-21-LF16-NFB) interfaces to a syringe pump and is 1/4 in. NPT tapped to receive a male 1/4 in. NPT threaded pressure transmission line. One 1.18 mm diameter hole was drilled completely through the long axis center of other solid endcap (Part No. 20-21-LF16-C) to allow NMR tank circuit access to the pressure space. Four more shallow holes were drilled on the outer circumference of the stainless steel endcap and 10–32 tapped to connect the 2 in. copper pipe endcap and cylindrical pipe section that houses the NMR detection circuit capacitors. A photograph of the HiP-NMR probe showing the HiP stainless steel reactor with endcaps and the copper NMR circuit housing is provided in Fig. 1(a). The schematic drawing of the HiP-NMR probe in Fig. 1(b) shows some relevant dimensions, the HiP reactor and endcaps, the copper pipe containing the capacitors for the NMR circuit, and a press fit tubular plastic coil form that sleeves into the HiP reactor. The NMR detection coil is mounted at the end of this 1.4 cm outer diameter, 0.94 cm inner diameter tubular plastic coil form as shown in the photograph in Fig. 1(c) and the schematic drawing in Fig. 1(d). Coil forms were constructed from several different plastics in anticipation of unwanted background signals and reactivity to chemicals and pressure. To date coil forms made from teflon, delrin and polyvinylchloride performed the same with no evidence of background signals, reactivity to chemicals and deformity due to pressure. The plastic tube length is adjusted so that the NMR detection coil is centered in the pressure reactor and placed close to the wall of the pressure reactor to maximize sample volume inside of the solenoid coil thus improving detected signal amplitude. The solenoid coil is typically wrapped with Kapton tape to prevent electrical arcs to the pressure reactor wall. The 28 gauge, 21 turn, L = 6.8 μH, Berylco – 25 solenoid NMR detection coil has 32 cm long leads threading through and Stycast/Al_2O_3 epoxy sealed into the stainless steel endcap. These leads connect to the capacitors in the copper pipe ground shield to create the NMR tank circuit. Berylco – 25 was used to prevent the extrusion at high pressure commonly observed with copper wire. The consequence of this choice is that the coil plus lead resistance R = 3.4 Ω is extremely high and thus the circuit quality factor Q is low in comparison to using copper to construct an identical NMR detection coil with long leads.

Before putting the HiP-NMR probe near any human beings and delicate instrumentation it is important to make sure the pressure reactor can still be safely operated at the target pressures. This is a critical effort because the hole drilled in the pressure reactor end cap violates any safety information for the pressure reactor provided by HiP. Experience dealing with these modifications to HiP pressure reactors reveals that the reactor can safely maintain pressure up to 80% of the HiP maximum quoted operating pressure.

3. Materials and methods

The pure polydimethylesiloxane (PDMS) or Dow Corning® 200 Fluid with 50 CS was used as received from Dow Corning. Stycast epoxy was obtained from Lake Shore Cryotronics, Inc.

Application of the NMR pulse sequences shown in Fig. 2 and acquisition of the associated transient signals were accomplished

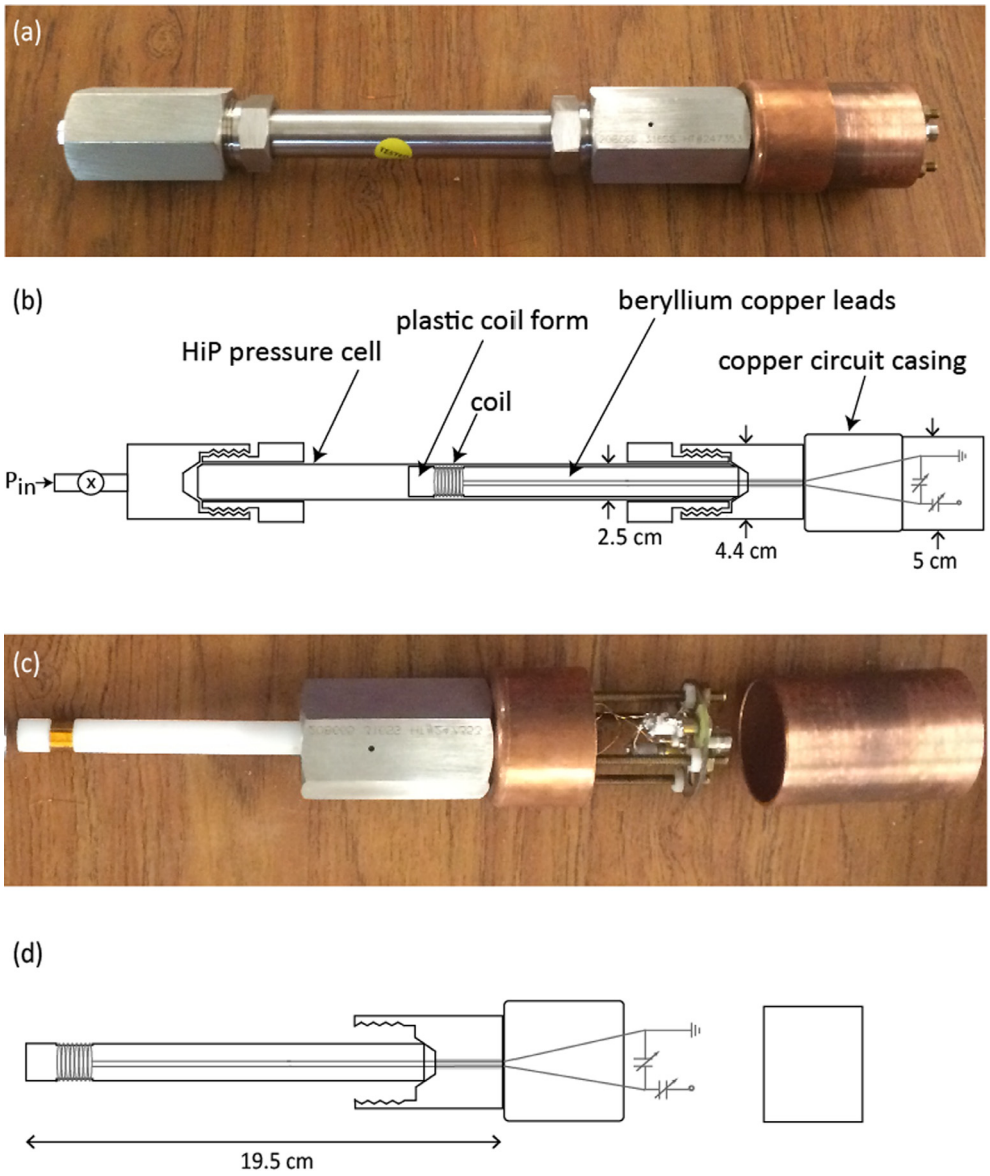

Fig. 1. Schematics and pictures of the HiP-NMR probe. The stainless steel HiP pressure reactor is on the left and the added copper NMR circuit ground shield is on the right in the photograph of the HiP-NMR probe shown in (a). A schematic of the probe showing the plastic coil sleeve is provided in (b). The Berylco – 25 coil, plastic sleeve, and NMR detection circuit in the photograph in (c) are drawn in the schematic (d).

using a Tecmag Redstone NMR spectrometer. The timing diagram shown in Fig. 2(a) combines an inversion recovery and Carr-Purcell-Meiboom-Gill (CPMG) pulse sequence together to correlate T_1 with T_2^{cpmg} while the timing diagram shown in Fig. 2(b) combines the two – pulse spin echo and CPMG pulse sequences together to correlate T_2^{echo} with T_2^{cpmg}. These two pulse sequences were used to track the correlation of these parameters as a function of pressure for ^{1}H nuclei in PDMS at two different magnetic field strengths and geometries. In both of these experiments, 200 acquisitions for each t_1 point were averaged and a 7.1 μs long, π/2 radio frequency (rf) pulse along with n = 1000, π rf pulses separated by dt_2 = 820 μs and detection of the spin echo maximum with 40 digitized points sampled every dt_3 = 6.3 μs were used. The T_1/T_2^{cpmg} pulse sequence in Fig. 2(a) used 40 t_1 points with a dt_1 = 30 ms dwell time while the T_2^{echo}/T_2^{cpmg} pulse sequence in Fig. 2(b) used 40 t_1 points with dt_1 = 2 ms. A 3.5 s recycle delay was used in all pulse sequences to insure that the magnetization recovered to thermal equilibrium prior to each scan and to avoid sample heating by reducing the RF-on duty cycle to 0.3% in these experiments.

Two magnets were used in this study because they are the ideally suited for portable NMR using non-traditional probe geometries like the new HiP-NMR probe. One magnet is a 107 mT, 1.5 cm standoff, single sided, linear magnet array with an associated 4.57 MHz ^{1}H Larmor frequency [17] while the other is a 123 mT, 1.8 cm standoff, single sided, cylindrical magnet array with an associate 5.25 MHz ^{1}H Larmor frequency [18].

Pressure was established inside of the NMR probe with a home-built syringe pump pressure system created from commercially available HiP parts. The system uses two in-line transducers to measure and monitor the pressure generated and stored in the pressure system and the HiP-NMR probe. All pressures are within ±2% of the quoted value. Caution must be used in the choice of pressure transmission fluid to avoid sample miscibility issues. Water was used as the pressure transmission fluid for all experiments reported here.

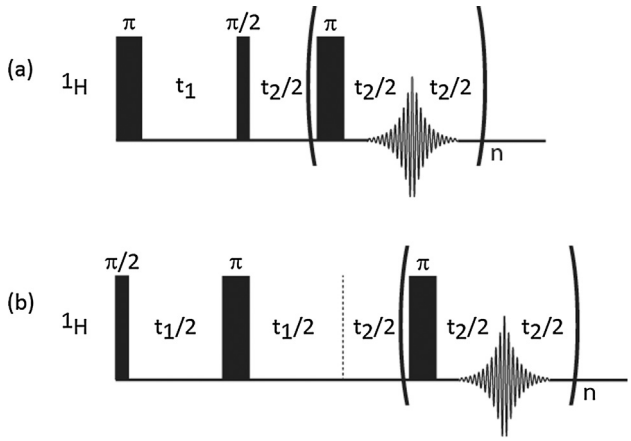

Fig. 2. Timing diagrams for the NMR pulse sequences. The coupling of the inversion recovery with the CPMG pulse sequence in (a) and the spin echo with the CPMG pulse sequence in (b) respectively provided ^{1}H T_1/T_2^{cpmg} and T_2^{echo}/T_2^{cpmg} correlation data as a function of pressure for this work.

All calculations and data processing were accomplished with laboratory developed Matlab software.

4. Results

The photographs in Fig. 3 show the HiP-NMR probe interfaced to the two magnets used in this study. ^{1}H NMR data were obtained using the linear magnet array in Fig. 3(a) or the cylindrical magnet array in Fig. 3(b). All NMR experiments were performed at radio frequencies between 4.6 and 5.3 MHz. The high resistance of the Berylco – 25 wire yields a circuit quality factor of Q = 6.6 as measured from the reflection coefficient in the usual way [19]. Despite having such a low Q value, the circuit has surprising rf power handling efficiency and delivers reasonable signals as typically 80 W of rf power yields a 7.1 μs π/2 rf pulse width and only modest signal averaging is required to obtain useful signal – to – noise ratios.

Examples of two dimensional ^{1}H relaxation correlation plots obtained using the HiP-NMR probe loaded with PDMS and pressurized to 100 MPa are provided in Fig. 4. The T_1/T_2^{cpmg} correlation shown in Fig. 4(a) was generated by applying a two dimensional inverse Laplace transform (ILT) to transient signals created with the pulse sequence in Fig. 2(a). A two dimensional ILT of the transient signals provided by the pulse sequence in Fig. 2(b) yields the T_2^{echo}/T_2^{cpmg} correlation shown in Fig. 4(b). Regardless of unilateral magnet or pressure choice, application of the pulse sequences in Fig. 2(a) and (b) to PDMS always generated just one peak following a two dimensional ILT. Summaries of the pressure and magnet dependence of the T_1/T_2^{cpmg} and T_2^{echo}/T_2^{cpmg} cross peak position are provided in Figs. 5 and 6 respectively. The square and circle icons

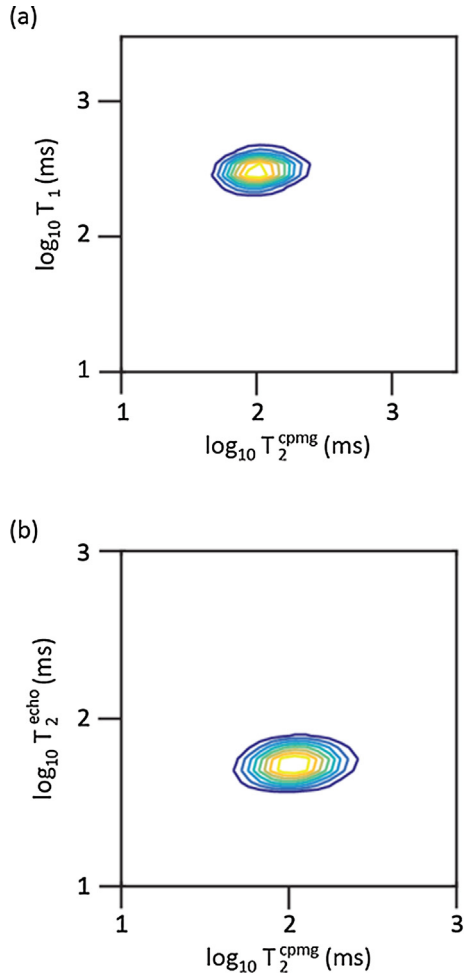

Fig. 4. Two dimensional ILT processed ^{1}H relaxation correlation data. This PDMS data was obtained using the linear magnet array at 100 MPa pressure. The ILT is used to convert the raw transient signals produced by the pulse sequences in Fig. 2 (a) and (b) to the respective T_1/T_2^{cpmg} and T_2^{echo}/T_2^{cpmg} correlations in (a) and (b).

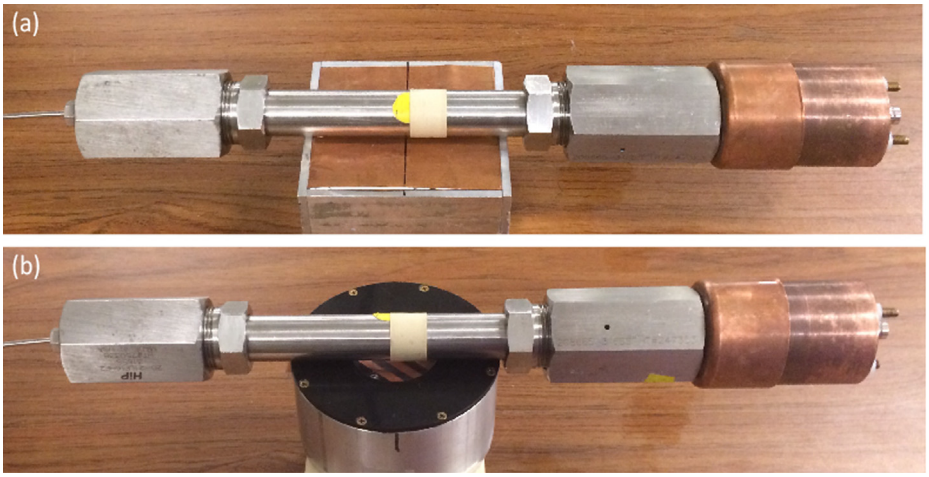

Fig. 3. HiP-NMR probe with unilateral magnets. The HiP-NMR probe is easy to use. Simple placement on the linear magnet array in (a), or on the cylindrical magnet array in (b) leads to measureable signals.

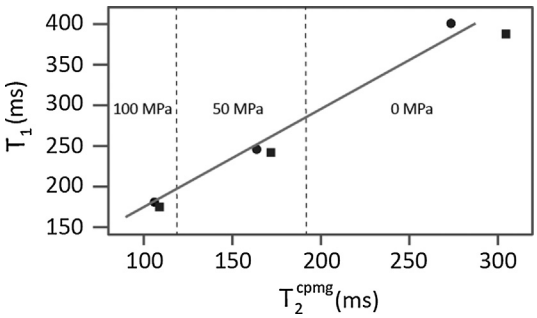

Fig. 5. Summary of the ^{1}H T_1/T_2^{cpmg} cross peak position in PDMS as a function of pressure and magnet. The squares and circles respectively correspond to measurements obtained from the linear and cylindrical magnet arrays. The gray line is included as a guide to the eye.

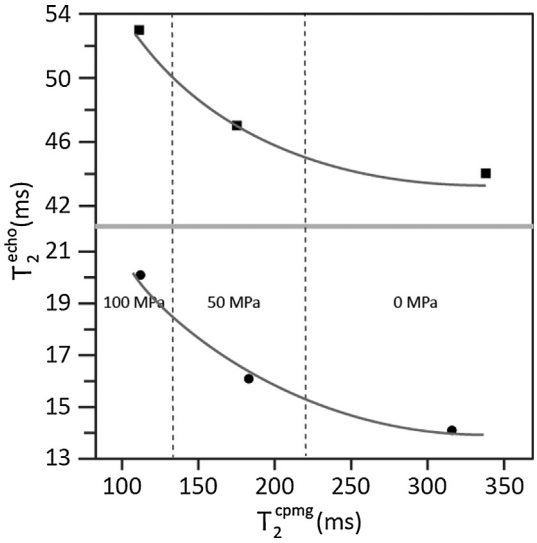

Fig. 6. Summary of the ^{1}H T_2^{echo}/T_2^{cpmg} cross peak position in PDMS as a function of pressure and magnet. The squares and circles respectively correspond to measurements obtained from the linear and cylindrical magnet arrays. The gray lines are included as a guide to the eye.

in these plots label the cross peak position observed with the linear magnet array in Fig. 3(a) and the cylindrical magnet array in Fig. 3 (b) respectively. Since there is just one peak in all of the two dimensional relaxation correlation plots a simple two dimensional exponential fit was used to more accurately determine the cross peak position. This analysis approach produced the cross peak positions shown in Figs. 5 and 6.

5. Discussion

The HiP-NMR probe design is simple and can be built from commercially available parts and standard non – magnetic capacitors common to an NMR laboratory. Moreover the probe can be used in any magnet system as long as the HiP reactor fits in the magnet and the static magnetic field is directed perpendicular to the symmetry axis of the NMR detection solenoid coil and long axis of the pressure reactor. This study considered portable unilateral magnet geometries that fulfill these requirements. Helmholtz geometry electromagnets and permanent magnet based magnetic resonance imaging instruments fulfill both these requirements as well. Although the bore diameter of standard cryogenically cooled solenoid magnets used for NMR spectroscopy may in certain cases accommodate the HiP-NMR probe, the static magnetic field direction is parallel to the long axis of the pressure cell making excitation and detection of traditional NMR signals impossible. One could replace the solenoid coil in the current HiP-NMR probe with a Helmholtz, split solenoid or a modified Alderman-Grant coil that places the rf field perpendicular to the long axis of the pressure cell in order to interface with a cryogenic solenoid magnet. Although the lower inductance of the coils used in this modified design would be easier to tune at the higher Larmor frequencies common to cryogenic magnets, the rf field would be seriously attenuated by the production of eddy currents in the ground shield that is in near physical contact with the rf coil. In contrast, the same effect can focus and enhance the rf field in the sample when a solenoid coil is parallel to the long axis of the pressure reactor.

It is surprising that the primary limitation in the overall probe design is not the 316 stainless steel used to construct the entire HiP pressure reactor. To date, there have been no problems with either signal acquisition from samples in the pressure reactor or from the HiP-NMR probe magnetizing and becoming stuck in or on an NMR magnet. Presumably this is because 316 stainless steel is largely non – magnetic unless elevated to high temperature by machining. In the cases reported here the strongest part of the magnetic field is across the center of the pressure reactor tube far from the machined endcaps and threads. In this way the most magnetically susceptible pressure reactor parts are kept in relatively low to zero magnetic field as shown by the photographs in Fig. 3. The primary limitation of the HiP-NMR probe is related to the use of Berylco-25 wire for the NMR detection coil and the ca. 32 cm long leads between the NMR tuning capacitors and the NMR detection coil mounted in the center of the pressure space and shown in Fig. 1(d). Berylco – 25 wire was chosen for one reason as mentioned above. A mixture of Stycast epoxy and Al_2O_3 maintains a pressure seal for a 28 gauge Berylco – 25 wire threading through a 1.8 mm diameter hole in stainless steel, tungsten carbide or beryllium copper alloy up to 3 GPa [10]. The consequence of this choice is that the coil – plus – lead resistance climbs to 3.4 Ω and the circuit quality factor drops to Q = 6.6. The poor Q value is not a problem for NMR excitation as 7.1 μs ^{1}H π/2 pulses are possible. The high resistance of the Berylco – 25 wire impacts the experiment in two ways. First, most of the 80 W of applied rf power is being dropped into the 3.4 Ω wire resistance thus local sample heating is possible. Care must be taken to make sure the pulse duty cycle is low enough to prevent this effect. This is not a problem for most protonated samples of interest where T_1 is typically greater than 100 ms. Second, the high wire resistance reduces the reception of the NMR free precession signal as the measured signal voltage is proportional to Q. It was recently shown that 28 gauge enameled copper wire Stycast epoxy/Al_2O_3 sealed into a 1.18 mm diameter hole in beryllium copper alloy resists extrusion up to 800 MPa [8]. Since the maximum operating pressure of the Micro Reactor family of HiP products is at most 450 MPa a new endcap/coil form assembly is being constructed with 28 gauge enameled copper wire. This alone will drop the wire resistance by a factor of five, and increase the Q by a factor of five thus decreasing the rf power demand and thermal dissipation while increasing the measured NMR signal intensity. The long leads between the NMR circuit capacitors and the NMR detection coil are not desirable, but were chosen because of simplicity and the fact that extra lead inductance does not introduce circuit tuning issues at Larmor frequencies below 10 MHz. Other coil coupling strategies were considered such as mounting the capacitors directly on the coil, inductively coupling to a remote coil and resonating the pressure reactor itself. It was decided that these other approaches, although superior in some ways, lacked the durability and simplicity known to work in extreme pressure environments and with realistic, heterogeneous, sometimes reactive samples.

The HiP-NMR probe is straightforward to use. Typically a valve is place between the NPT threaded pressure reactor endcap and the syringe pump. Thus, the HiP-NMR probe can be pressurized prior to placement on the single sided magnets as shown in Fig. 3(a) and (b). Although this approach may be more desirable as the estimate of real time pressure dependent dynamics by NMR is made possible, it can be problematic from a signal detection point of view. The HiP pressure reactor also serves as the HiP-NMR probe ground shield. Operation of the HiP-NMR probe with the syringe pump connected introduces noise at certain frequencies. In these cases, additional effort must be placed on the removal of ground loops between the NMR spectrometer, pressure transducers, and other associated electronics as well as making sure all components share a common direct path to ground.

Despite the low Q value of the NMR detection circuit due to Berylco – 25 wire, the HiP-NMR probe was more than able to provide useful relaxometry data. Two NMR experiments at three different pressures were performed on PDMS in order to demonstrate the function, performance, and potential usefulness of the HiP-NMR probe. PDMS is an ideal sample for this work. It is a known lubricant with pressure dependent macroscopic properties and a reasonable proton density and spin lattice relaxation time that yields a strong signal with minimal signal averaging.

5.1. T_1/T_2^{cpmg} ^1H relaxation correlation in PDMS

As mentioned above, application of the pulse sequence in Fig. 2 (a) to a sample of PDMS at 100 MPa applied pressure leads to the correlation between PDMS ^1H T_1 and T_2^{cpmg} values following an ILT as shown in Fig. 4(a). This data was recorded using the linear magnet array. The plot in Fig. 5 shows the T_1/T_2^{cpmg} cross peak position as a function of pressure for the two different unilateral magnets. The gray line is included to guide the eye and illustrate that at all pressures $T_1 \approx T_2^{cpmg}$. Closer inspection reveals that at all pressures T_1 is slightly greater than T_2^{cpmg}, suggesting that the static field gradients established by both unilateral magnets are so large that the $dt_2 = 820$ μs CPMG π pulse delay is too long to completely remove all diffusion contributions to T_2^{cpmg}. The discrepancy between T_1 and T_2^{cpmg} is larger for the cylindrical magnet array than for the linear magnet array suggesting that the persistent static magnetic field gradient for the cylindrical array is greater than for the linear array. The fact that $T_1 \approx T_2^{cpmg}$ suggests that the extreme narrowing limit applies and that the correlation time of the motion τ_c is less than the inverse of the Larmor frequency $\tau_c < 1/\omega_0$ at all pressures. The decrease in T_1 and T_2^{cpmg} values with pressure is also expected. As pressure increases, the PDMS viscosity and τ_c also increase. Since, in the extreme narrowing limit $T_1 \approx T_2^{cpmg} \propto 1/\tau_c$, the T_1 and T_2^{cpmg} values decrease with added pressure.

5.2. T_2^{echo}/T_2^{cpmg} ^1H relaxation correlation in PDMS

As mentioned above, application of the pulse sequence in Fig. 2 (a) to a sample of PDMS at 100 MPa pressure leads to the correlation between PDMS ^1H T_2^{echo} and T_2^{cpmg} values following an ILT as shown in Fig. 4(b). This data was recorded using the linear magnet array. The plot in Fig. 6 shows the behavior of the T_2^{echo}/T_2^{cpmg} cross peak position as a function of pressure for the two unilateral magnets. Again the gray lines are included to guide the eye. As expected with reference to Fig. 5, the T_2^{cpmg} value in Fig. 6 drops with pressure in the same way suggesting that the PDMS viscosity increases with pressure since the extreme narrowing limit applies and $T_2^{cpmg} \propto 1/\tau_c$. The increase in the T_2^{echo} value with pressure on both magnets is also consistent with increased PDMS viscosity with pressure. The value of T_2^{echo} intimately depends on static magnetic field gradient strength and macroscopic diffusion. The attenuation of diffusion effects enjoyed by T_2^{cpmg} due to the application of many π rf pulses is not shared by T_2^{echo} where just one π rf pulse is applied. The greater difference between T_1 and T_2^{cpmg} values obtained using the cylindrical magnet array in Fig. 5 that was attributed to a larger static magnetic field gradient for the cylindrical magnet array versus the linear magnet array is much more pronounced in the magnet dependence of T_2^{echo} values at all pressures in Fig. 6. The increase in T_2^{echo} values obtained with both magnets with pressure is consistent with increased viscosity at pressure. The increased pressure lowers the macroscopic diffusion coefficient, attenuating the effect of diffusion on the spin echo amplitude thus increasing T_2^{echo}. The idea that the static magnetic field gradient is larger for the cylindrical magnet array than for the linear magnet array is illustrated by the nearly a factor of two difference between T_2^{echo} values obtained from these magnets at all pressures.

6. Conclusion

The design, construction and performance of a simple NMR probe capable of studying the pressure dependence of the fundamental NMR relaxometry parameters for realistic, heterogeneous samples was described. The HiP-NMR probe simplicity, dependence on readily available parts, and ability to conform to many portable magnet geometries, provides a low cost avenue to the characterization of many industrial processes at elevated pressure such as high pressure food processing and the downhole performance of oil well drilling muds. The primary limitation of the current HiP-NMR probe is the use of Berylco – 25 wire that lowers the NMR detection circuit Q and thus the detected signal intensity. Another version of the HiP-NMR probe, currently under construction, replaces this wire with enameled copper to increase the circuit Q and probe sensitivity. Although not stable to 3 GPa, the use of copper wire should not be problematic until 800 MPa, a pressure above the maximum operating pressure of this family of HiP pressure reactors. Ongoing work involves using NMR relaxometry, portable magnets and the HiP-NMR probe to study industrially relevant samples like high pressure processed foods, oil well drilling mud, and consumable materials at pressure like shaving cream. Hopefully, this simple HiP-NMR probe design will make these types of samples and others not yet identified accessible to an inexpensive NMR study for the first time.

Declaration of Competing Interest

None.

Acknowledgement

Support for this work from the Center for Process Analysis and Control at the University of Washington is gratefully acknowledged.

References

[1] L. Ballard, C. Reiner, J. Jonas, High-resolution NMR probe for experiments at high pressures, J. Magn. Reson. A 123 (1996) 81–86.
[2] J. Jonas, Nuclear magnetic resonance measurements at high pressure, Rev. Sci. Instrum. 43 (1972) 643–649.
[3] J. Jonas, P. Kozoil, X. Peng, C. Reiner, D.M. Campbell, High resolution NMR spectroscopy at high pressures, J. Magn. Reson, B 102 (1993) 299–309.
[4] Daedelus Innovations. http://www.daedalusinnovations.com.
[5] J.L. Urbauer, J.H. Short, L.K. Dow, A.J. Wand, Structural analysis of a novel interaction by calmodulin: high-affinity binding of a peptide in the absence of calcium, Biochemistry 34 (1995) 8099–8109.

[6] R.W. Peterson, A.J. Wand, Self-contained high-pressure cell, apparatus, and procedure for the preparation of encapsulated proteins dissolved in low viscosity fluids for nuclear magnetic resonance spectroscopy, Rev. Sci. Instrum. 76 (2005) 094101-1–094101-7.
[7] C. Charlier, T.R. Alderson, J.M. Courtney, J. Ying, P. Anfinrud, A. Bax, Study of protein folding under native conditions by rapidly switching the hydrostatic pressure inside an NMR sample cell, Proc. Natl. Acad. Sci. 115 (18) (2018) E4169–E4178, https://doi.org/10.1073/pnas.1803642115.
[8] B.G. Pautler, C.A. Colla, R.L. Johnson, P. Klavins, S.J. Harley, C.A. Ohlin, D.A. Sverjensky, J.W. Walton, W.H. Casey, A high-pressure NMR probe for aqueous geochemistry, Angew. Chem. 126 (2014) 9946–9949.
[9] G. Ochoa, C.D. Pilgrim, M.N. Martin, C.A. Colla, P. Klavins, M.P. Augustine, W.H. Casey, ^{2}H and ^{139}La NMR spectroscopy in aqueous solution at geochemical pressures, Angew. Chem. 127 (2015) 15664–15667.
[10] M.P. Augustine, G. Ochoa, W.H. Casey, Steps to achieving high-resolution NMR spectroscopy on solutions at GPa pressure, Am. J. Sci. 317 (2017) 846–860.
[11] S.-H. Lee, K. Luszczynski, R.E. Norberg, NMR in a diamond anvil cell, Rev. Sci. Instrum. 58 (1987) 415–417.
[12] H. Han, M. Ouellette, B. MacMillan, F. Goora, R. MacGregor, D. Green, B.J. Balcom, High pressure magnetic resonance imaging with metallic vessels, J. Magn. Reson. 213 (2011) 90–97.
[13] R. Freedman, V. Anand, B. Grant, K. Ganesan, P. Tabrizi, R. Torres, D. Catina, D. Ryan, C. Borman, C. Krueckl, A compact high-performance low-field NMR apparatus for measurements on fluids at very high pressures and temperatures, Rev. Sci. Instrum. 85 (2014) 025102-1–025102-10.
[14] M. Shakerian, B.J. Balcom, A MR/MRI compatible core holder with RF probe immersed in containing fluid, J. Magn. Reson. 286 (2018) 36–41.
[15] M. Muntean, O. Marian, V. Barbieru, G.M. Cătunescu, O. Ranta, I. Drocas, S. Terhes, Agric. Agric. Sci. Procedia 10 (2016) 377–383.
[16] A.E. Marble, I.V. Mastikhin, B.G. Golpitts, B.J. Balcom, A compact permanent magnet array with a remote homogeneous field, J. Magn. Reson. 186 (2007) 100–104.
[17] J.C. García-Naranjo, P. Guo, F. Marica, G. Liao, B.J. Balcom, Magnetic resonance core-plug analysis with the three-magnet array unilateral magnet, Petrophysics 55 (2014) 229–239.
[18] S. Utsuzawa, E. Fukushima, Unilateral NMR with a barrel magnet, J. Magn. Reson. 282 (2017) 104–113.
[19] C.-N. Chen, D.I. Hoult, Biomedical Magnetic Resonance Technology, Adam Hilger, New York, 1989.